Materials Research. 2015; 18(Suppl 2): 2-7
DOI: http://dx.doi.org/10.1590/1516-1439.320614

Characterization of Nd^{3+}-doped Tellurite Glasses with Low OH Content

Francine Bettio Costa[a], Keizo Yukimitu[a], Luiz Antonio Oliveira Nunes[b],

Luis Humberto da Cunha Andrade[c], Sandro Marcio Lima[c], João Carlos Silos Moraes[a]*

[a]Universidade Estadual Paulista – UNESP, Avenida Brasil, 56, Centro, CEP 15385-000, Ilha Solteira, SP, Brazil
[b]Instituto de Física de São Carlos – IFSC, Avenida Trabalhador Sancarlense, 400, Parque Arnold Schimidt, CEP 13563-120, São Carlos, SP, Brazil
[c]Universidade Estadual de Mato Grosso do Sul – UEMS, Cidade Universitária de Dourados, CP 351, CEP 79804-970, Dourados, MS, Brazil

Received: August 29, 2014; Revised: June 16, 2015

This work presents the results of the investigation of structural and thermal properties of Nd^{3+}-doped tellurite glasses with low OH content. The samples were characterized by XRD, FTIR, DTA, UV/VIS/NIR and Archimedes' method. Tellurite glasses of composition $(100-x)(0.8TeO_2 + 0.2WO_3) + xNd_2O_3$ ($x = 0$, 0.05, 0.5, 1, 2, and 4 mol%) were prepared in both ambient and oxygen atmospheres. All samples showed an increase of the values of T_g, T_x, and T_x-T_g with Nd_2O_3 addition. The reduction of OH content implies a slight decrease of T_g. The density and the molar volume of the glasses increased with Nd_2O_3. The intensity of the absorption bands associated with Te-O bonds of TeO_4 units decreased compared with the bands associated with Te-O bonds of $TeO_{3+1/3}$ units. This indicates that Nd_2O_3 favors the transformation of the TeO_4 groups in TeO_3 groups via TeO_{3+1}, increasing the NBOs and contributing to the formation of strongly hydrogen-bonded OH groups. The samples made in O_2 showed a reduction of 48% of "free" OH ions compared with the Amb ones.

Keywords: *tungsten-tellurite glasses, rare-earth, low OH content*

1. Introduction

Tellurite glasses combine the attributes of reasonable thermal stability, high refractive index, high solubility of rare earth (RE) ions, larger absorption and emission cross-sections, and low phonon energy compared to the silicate, phosphate, and borate glasses[1,2], with a wide transmission window in the infrared region[2]. In particular, tungsten-tellurite glasses have higher phonon energy and a higher glass transition temperature compared to the other tellurite glasses; therefore, they can be used at high optical intensities without exposure to thermal damage[3]. The RE-doped tungsten-tellurite glasses have been shown to have excellent properties for applications such as planar waveguides[4], amplifiers[5], and lasers[6,7]. Several RE ions have been studied for laser application. Among them, the Nd^{3+} ion is one of the most investigated. This is due to the high quantum efficiency of the $^4F_{3/2} \rightarrow {}^4I_{11/2}$ emission transition near 1060 nm. Lasing has been obtained in different bulk glasses doped with Nd^{3+} ions[6-10]. However, tellurite glasses have larger amounts of water when melted in air. The water is incorporated into the glass as hydroxyl (OH) groups, which have a strong and broad vibrational absorption band between 2000 and 3600 cm^{-1}, promoting energy loss. The absorption losses due to the OH groups are disadvantageous because they decrease luminescence quantum efficiency, hindering the practical use of these glasses[11-13].

In this paper, we investigate the thermal and structural properties of the Nd^{3+}-doped tungsten-tellurite glasses according to neodymium concentration, with samples prepared in ambient and oxygen atmospheres.

2. Experimental

Tungsten-tellurite glasses with nominal composition $(100-x)(0.8TeO_2 + 0.2WO_3) + xNd_2O_3$, where $x = 0$, 0.05, 0.5, 1, 2, and 4 mol%, were prepared by conventional melt-quenching method in two different atmospheres: ambient (Amb) and oxygen (O_2). Table 1 shows the nominal composition (mol%) and molar mass (g/mol) of the glasses. The reagents (with > 99% or higher purity) were weighed and mixed into an agate mortar.

For the set prepared in the Amb atmosphere, the mixture of reagents was melted in a platinum crucible at 880 °C for 30 minutes. The melt was poured into a stainless-steel mold, pre-heated near the glass transition temperature (~350 °C). For the set prepared in the O_2 atmosphere, the same procedures were carried out, except that the furnace was placed inside a sealed camera, where a vacuum was created. This was followed by an injection of O_2 (until the inner pressure reached 1 atm). After their contents were poured, the glasses were returned to the other furnace for annealing. The annealing lasted for 2 hours at 350 °C and then the sample was slowly cooled to room temperature. The produced glasses were cut and polished, reaching thicknesses between 0.71 and 0.95 mm.

*e-mail: joca@dfq.feis.unesp.br

The glassy state in these samples was confirmed by X-ray diffraction (XRD) analysis using Cu K_α radiation. Glass transition (T_g) and crystallization onset (T_x) temperatures were measured using the differential thermal analysis (DTA) technique at a heating rate of 10 °C/min. The absorption spectra in the range of 400 to 700 nm were obtained using a Perkin Elmer Lambda 900 UV/VIS/NIR spectrophotometer. The densities of the samples were determined by Archimedes' method, using distilled water as the immersion liquid. The absorption spectra were recorded in the range of 400 to 1000 cm^{-1} for the powder samples and in the range of 2000 to 4000 cm^{-1} for the bulk samples using an N_2 purge, and were obtained by Fourier transform infrared (FTIR) spectroscopy using a Nicolet Nexus 670 FTIR spectrometer.

3. Results and Discussion

The XRD curves of the undoped and Nd^{3+}-doped TW glasses prepared in both atmospheres presented two halos that confirm the amorphous nature of the glasses.

The DTA analyses were performed to determine the thermal behavior of the prepared glasses. The DTA curves of the glasses prepared in Amb and O_2 atmospheres are shown in Figures 1a and 1b, respectively. The T_g and T_x increase as a function of the Nd_2O_3 concentration. The increase of the T_g can be explained by the increase in the molar mass (Table 1). It could also be due to the high bond energy of the Nd-O (703 kJ/mol) compared to Te-O (376 kJ/mol) and W-O (672 kJ/mol), and due to the increase in the average crosslink density (Table 1), explained by replacement of the TeO_2 (coordination numbers 3 and 4) and WO_3 (coordination number 4 or 6) for Nd_2O_3 (in general, coordination number 8), which may be assigned to the creation of a more compact structure[14].

The average crosslink density was calculated according to Equation 1, where x_i is the mol fraction of component oxide; n_c is the crosslink density per cation, which is equal to $n_f - 2$, with n_f being the coordination number of cation; and N_c is the number of cations per glass formula unit.

Table 1. Nominal composition (mol%), mass molar (g/mol), and average crosslink density of the Nd^{3+}-doped TW glasses.

Sample	TeO_2 (mol%)	WO_3 (mol%)	Nd_2O_3 (mol%)	MM (g/mol)	$\overline{n_c}$
TW	80	20	0	174.05	2.40
TW-0.05Nd	79.96	19.99	0.05	174.13	2.40
TW-0.5Nd	79.6	19.9	0.5	174.86	2.44
TW-1Nd	79.2	19.8	1.0	175.67	2.47
TW-2Nd	78.4	19.6	2.0	177.30	2.54
TW-4Nd	76.8	19.2	4.0	180.54	2.68

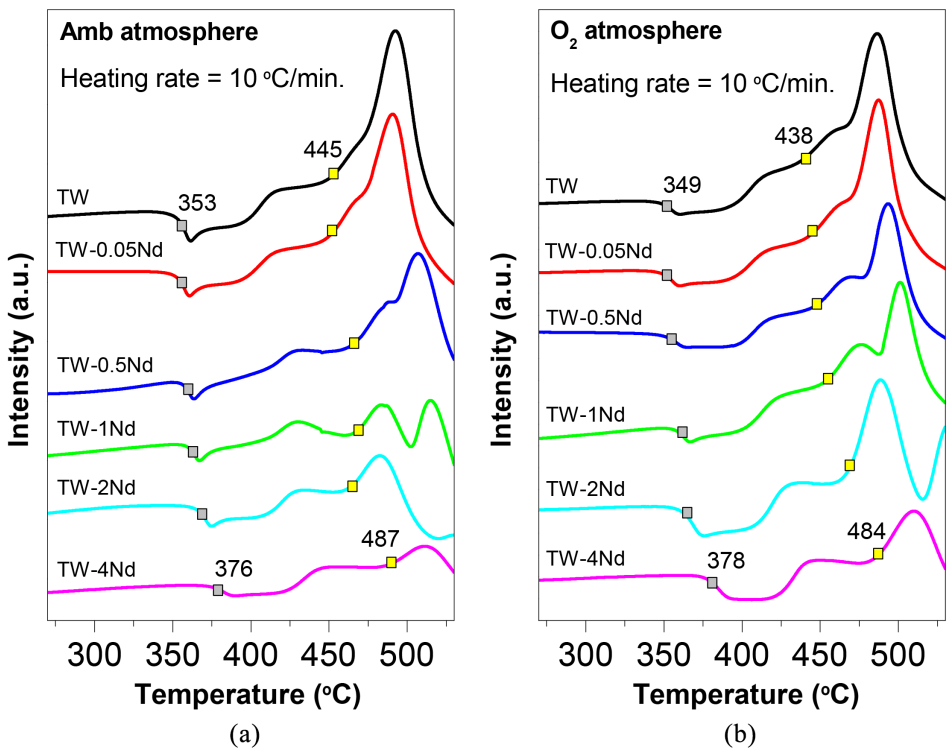

Figure 1. DTA curves of the undoped and Nd^{3+}- doped TW glasses prepared in: (a) Amb and (b) O_2 atmospheres.

$$\overline{n_c} = \frac{\sum_i x_i (n_c)_i (N_c)_i}{\sum_i x_i (N_c)_i} \quad (1)$$

Comparing atmospheres, the T_g in the Amb atmosphere is slightly greater than in O_2 atmosphere, because the glasses prepared in Amb present a higher number of OH groups, leading to significant intermolecular bond strength[15]. The temperature difference between the T_x and T_g (ΔT), indicates the thermal stability of the glass. The ΔT increased from 92 to 111 °C and from 89 to 106 °C for the glasses in Amb and O_2 atmospheres, respectively, depending on the addition of Nd_2O_3, indicating higher resistance to temperature variations.

Figures 2a and 2b show the IR absorption spectra of the glasses prepared in Amb and O_2 atmospheres, respectively, in the range of 400 to 1000 cm^{-1}. It was observed that the introduction of Nd_2O_3 to the glass led to variations in the glass network. The intensity of the absorption band centered at 495 cm^{-1}, which is associated with Te-O-Te/Te-O-W linkages of TeO_4 units, decreases and shifts to lower wavenumbers with the addition of Nd_2O_3. This suggests that the Nd_2O_3 addition favors the cleavage of such linkages and may form Te-O-Nd bonds[14]. Furthermore, the intensity of the absorption band centered at 649 cm^{-1}, which is associated with Te-O bonds of TeO_4 units, decreases compared with that associated with Te-O bonds of $TeO_{3+1/3}$ units located at 778 cm^{-1}[16–18]. This indicates that the conversion of TeO_4 to TeO_3 increases the TeO_3 isolated units with the non-bridging oxygen (NBO)[19], contributing to the formation of the Te-OH groups. The shoulder observed at 870 cm^{-1} is associated with W-O-W linkages, and the band at 942 cm^{-1} corresponds to W=O and W-O$^-$ bonds of WO_4 or WO_6 units[20]. The phonon energy of the TW glasses is 942 cm^{-1} and decreases slightly with Nd_2O_3 content.

Figure 3a shows the absorption spectra of the TW-0.05Nd and TW-4Nd glasses prepared in both atmospheres in the spectral range from 400 to 700 nm. The Nd_2O_3 addition causes a blue shift of the fundamental absorption edge tail (inset of Figure 3a). This shift has been observed in previous studies[14,21,22]. It has been related to the structural conversion from TeO_4 (tbp = *trigonal bipyramid*) to TeO_{3+1} and TeO_3 (tp = trigonal pyramid) units[21] and can be responsible for the color change of glasses from yellow to green (Figure 3b), since the luminescent emissions are outside of the visible region.

Density and molar volume increase with Nd_2O_3 addition (Table 2). This increase in density is because the molar mass of Nd_2O_3 (336.48 g/mol) is greater than that of TeO_2 and WO_3 (159.60 and 231.84 g/mol, respectively), increasing the molar mass of the doped glasses (Table 1). This increase in molar volume is probably due to an increase in the bond length between Te and O atoms resulting from the observed structural conversion ($TeO_4 \rightarrow TeO_3$)[23].

The inset of the Figure 4 gives the IR absorption spectra of the TW and TW-4Nd glasses, prepared in both atmospheres, in the range of 2000 to 3600 cm^{-1}, which are associated with OH$^-$ absorption. The spectra of the glasses exhibit a broad absorption band centered at 3160 cm^{-1} (with a shoulder at ~3300 cm^{-1}) and a weaker and sharper band

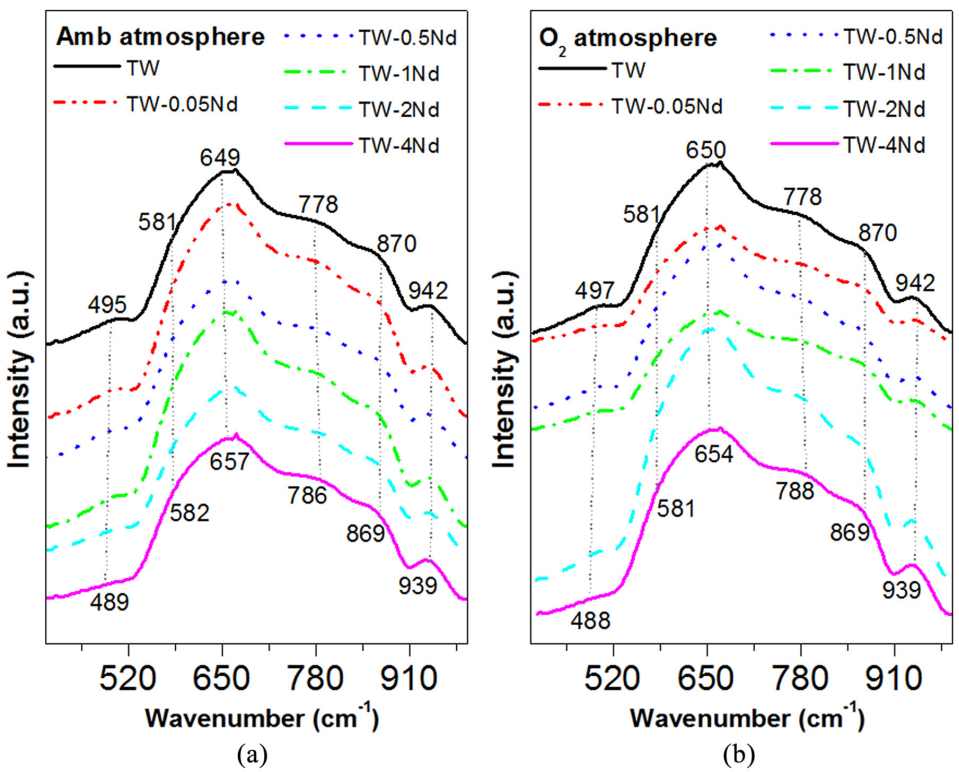

Figure 2. Absorption spectra in the range from 400 to 1000 cm^{-1} of the Nd^{3+}-doped TW glasses prepared in (a) Amb and (b) O_2 atmospheres.

Table 2. Density (g/cm^3) and molar volume (cm^3/mol) of the undoped and Nd^{3+}-doped TW glasses prepared in Amb and O_2 atmospheres.

Sample	ρ (g/cm^3)*		*MV* (cm^3/mol)	
	Amb	O_2	Amb	O_2
TW	5.89	5.88	29.55	29.60
TW-0.05Nd	5.89	5.88	29.56	29.61
TW-0.5Nd	5.89	5.89	29.69	29.69
TW-1Nd	5.89	5.89	29.83	29.83
TW-2Nd	5.93	5.92	29.90	29.95
TW-4Nd	5.94	5.93	30.39	30.45

*The density error is 0.02.

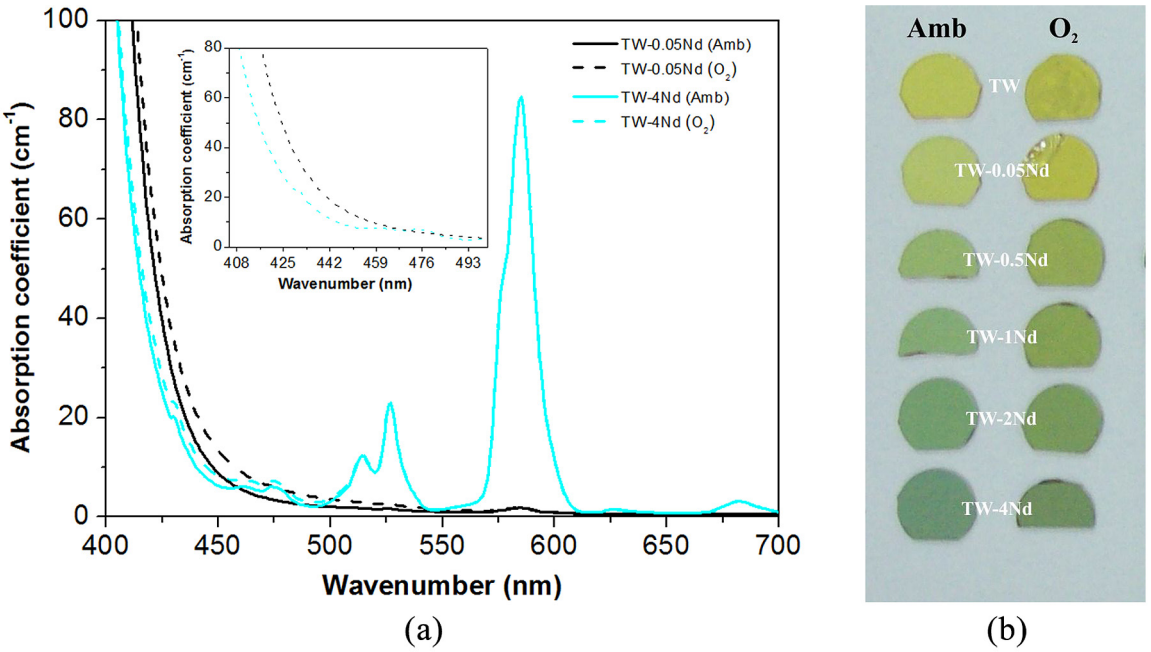

Figure 3. (a) Absorption spectrum of the TW-0.05Nd and TW-4Nd glasses and (b) Undoped and Nd^{3+}-doped TW glasses, in Amb and O_2 atmospheres.

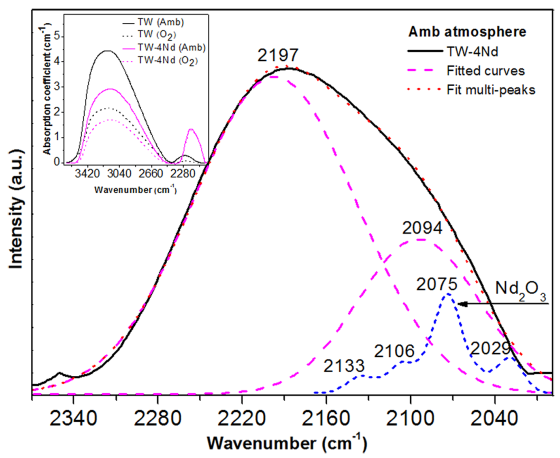

Figure 4. Deconvolution of the absorption band centered at 2200 cm^{-1} of the TW-4Nd glass prepared in Amb atmosphere and absorption spectra of the pure Nd_2O_3. The inset shows the OH absorption spectra of the samples prepared in both atmospheres.

between 2000 and 2400 cm^{-1} which are ascribed to the stretching mode of the weakly and strongly hydrogen-bonded Te-OH…O-Te groups, respectively[24,25]. The band around 3300 cm^{-1} is assigned to a combination of the free Te-OH groups and molecular water[25]. The broad absorption band at 3160 cm^{-1} has been used to assess the reduction of the OH content in the glasses[12,26]. The amplitude this absorption band of the samples prepared in O_2 atmosphere decreased by an average of 48%.

The amount of weakly hydrogen-bonded Te-OH…O-Te and free Te-OH groups/molecular water groups decreased with the addition of Nd_2O_3, whereas the number of strongly hydrogen-bonded Te-OH…O-Te groups increased. The same behavior is observed in the samples prepared in O_2 atmosphere. This is explained by an increase in the intensity of the absorption band at 2000–2400 cm^{-1}. The shift from higher to lower wavenumbers (74 cm^{-1}) of this band according to the Nd_2O_3 addition can be explained by the decrease of the O...O distances, since this addition causes an increase in the molar volume of the TW glass (Table 2) and, consequently, a

decrease of the free space in which the water impurities could reside[26]. The appearance of a shoulder is also observed in this band for TW-1Nd, TW-2Nd and TW-4Nd samples. The shift to lower wavenumbers led to a superposition of the strongly hydrogen-bonded band with weak bands of neodymium oxide, with a maximum at 2075 cm^{-1} (Figure 4). The deconvolution indicates only one absorption peak for TW, TW-0.05Nd, and TW-0.5Nd samples and two absorption peaks for the other doped samples, centered at ~2100 and ~2220 cm^{-1}. Thus, the shoulder observed at ~2100 cm^{-1} is assigned here to the neodymium. This shoulder also undergoes a shift of 24 cm^{-1} when the concentration of neodymium increases from 1 to 4 mol%, which is probably due to decreases of Nd-O bond length.

4. Conclusions

Measurements of DRX, DTA, UV/VIS/NIR, density, and FTIR, were performed for thermal and structural characterization of the undoped and Nd^{3+}-doped TW glasses prepared in Amb and O_2 atmospheres. We conclude that in each sample set, the increase of Nd in the TW matrix caused structural changes ($TeO_4 \rightarrow TeO_3$) and consequently increased the density, molar volume, T_g and ΔT. In addition, it caused a blue shift of the glass fundamental absorption edge tail.

References

1. Jha A, Richards B, Jose G, Teddy-Fernandez T, Joshi P, Jiang X, et al. Rare-earth ion doped TeO_2 and GeO_2 glasses as laser materials. *Progress in Materials Science*. 2012; 57(8):1426-1491. http://dx.doi.org/10.1016/j.pmatsci.2012.04.003.
2. Wang JS, Vogel EM and Snitzer E. Tellurite glass: a new candidate for fiber devices. *Optical Materials*. 1994; 3(3):187-203. http://dx.doi.org/10.1016/0925-3467(94)90004-3.
3. Çelikbilek M, Ersundu AE, Solak N and Aydin S. Investigation on thermal and microstructural characterization of the TeO_2-WO_3 system. *Journal of Alloys and Compounds*. 2011; 509(18):5646-5654. http://dx.doi.org/10.1016/j.jallcom.2011.02.109.
4. Conti GN, Berneschi S, Bettinelli M, Brenci M, Chen B, Pelli S, et al. Rare-earth doped tungsten tellurite glasses and waveguides: fabrication and characterization. *Journal of Non-Crystalline Solids*. 2004; 345-346:343-348.
5. Kuan PW, Li K, Zhang G, Wang X, Zhang L, Bai G, et al. Compact broadband amplified spontaneous emission in Tm^{3+}-doped tungsten tellurite glass double-cladding single-mode fiber. *Optical Materials Express*. 2013; 3(6):723-728. http://dx.doi.org/10.1364/OME.3.000723.
6. Kalaycioglu H, Cankaya H, Ozen G, Ovecoglu L and Sennaroglu A. Lasing at 1065 nm in bulk Nd^{3+}-doped telluride-tungstate glass. *Optics Communications*. 2008; 281(24):6056-6060. http://dx.doi.org/10.1016/j.optcom.2008.08.053.
7. Cankaya H and Sennaroglu A. Bulk Nd^{3+}-doped tellurite glass laser at 1.37 μm. *Applied Physics. B, Lasers and Optics*. 2010; 99(1-2):121-125. http://dx.doi.org/10.1007/s00340-009-3752-0.
8. Wang JS, Machewirth DP, Wu F, Snitzer E and Vogel EM. Neodymium-doped tellurite single-mode fiber laser. *Optics Letters*. 1994; 19(18):1448-1449. http://dx.doi.org/10.1364/OL.19.001448. PMid:19855548.
9. Lei N, Xu B and Jiang Z. Ti:sapphire laser pumped Nd: tellurite glass laser. *Optics Communications*. 1996; 127(4-6):263-265. http://dx.doi.org/10.1016/0030-4018(96)00099-5.
10. Iparraguirre I, Azkargorta J, Fernández-Navarro JM, Al-Saleh M, Fernández J and Balda R. Laser action and upconversion of Nd^{3+} in tellurite bulk glass. *Journal of Non-Crystalline Solids*. 2007; 353(8-10):990-992. http://dx.doi.org/10.1016/j.jnoncrysol.2006.12.103.
11. Ebendorff-Heidepriem H, Kuan K, Oermann MR, Knight K and Monro TM. Extruded tellurite glass and fibers with low OH content for mid-infrared applications. *Optical Materials Express*. 2012; 2(4):432-442. http://dx.doi.org/10.1364/OME.2.000432.
12. Wang PF, Li WN, Peng B and Lu M. Effect of dehydration techniques on the fluorescence spectral features and OH absorption of heavy metals containing fluoride tellurite glasses. *Journal of Non-Crystalline Solids*. 2012; 358(4):788-793. http://dx.doi.org/10.1016/j.jnoncrysol.2011.12.029.
13. Navarra G, Iliopoulos I, Militello V, Rotolo SG and Leone M. OH-related infrared absorption bands in oxide glasses. *Journal of Non-Crystalline Solids*. 2005; 351(21-23):1796-1800. http://dx.doi.org/10.1016/j.jnoncrysol.2005.04.018.
14. Kamalaker V, Upender G, Ramesh C and Mouli VC. Raman spectroscopy, thermal and optical properties of TeO2-ZnO-Nb2O5-Nd2O3 glasses. *Spectrochimica Acta. Part A: Molecular and Biomolecular Spectroscopy*. 2012; 89:149-154. http://dx.doi.org/10.1016/j.saa.2011.12.057. PMid:22261103.
15. Callister WD Jr. *Materials science and engineering: an introduction*. Hoboken: John Wiley & Sons; 2000.
16. Shaltout I, Tang Y, Braunstein R and Abu-Elazm AM. Structural studies of tungstate-tellurite glasses by raman spectroscopy and differential scanning calorimetry. *Journal of Physics and Chemistry of Solids*. 1995; 56(1):141-150. http://dx.doi.org/10.1016/0022-3697(94)00150-2.
17. Upender G, Bharadwaj S, Awasthi AM and Chandra Mouli V. Glass transition temperature-structural studies of tungstate tellurite glasses. *Materials Chemistry and Physics*. 2009; 118(2-3):298-302. http://dx.doi.org/10.1016/j.matchemphys.2009.07.058.
18. Hager IZ and El-Mallawany R. Preparation and structural studies in the (70-x)TeO_2-20WO_3-10Li_2O-xLn_2O_3 glasses. *Journal of Materials Science*. 2010; 45(4):897-905. http://dx.doi.org/10.1007/s10853-009-4017-3.
19. Jlassi I, Elhouichet H and Ferid M. Thermal and optical properties of tellurite glasses doped erbium. *Journal of Materials Science*. 2011; 46(3):806-812. http://dx.doi.org/10.1007/s10853-010-4820-x.
20. Ersundu AE, Çelikbilek M and Aydin S. Characterization of B_2O_3 and/or WO_3 containing tellurite glasses. *Journal of Non-Crystalline Solids*. 2012; 358(3):641-647. http://dx.doi.org/10.1016/j.jnoncrysol.2011.11.012.
21. Nazabal V, Todoroki S, Nukui A, Matsumoto T, Suehara S, Hondo T, et al. Oxyfluoride tellurite glasses doped by erbium: thermal analysis, structural organization and spectral properties. *Journal of Non-Crystalline Solids*. 2003; 325(1-3):85-102.
22. Liao G, Chen Q, Xing J, Gebavi H, Milanese D, Fokine M, et al. Preparation and characterization of new fluorotellurite glasses for photonics application. *Journal of Non-Crystalline Solids*. 2009; 355:447-452.

23. Hager IZ, El-Mallawany R and Bulou A. Luminescence spectra and optical properties of TeO2-WO3-Li2O glasses doped with Nd, Sm and Er rare earth ions. *Physica B: Condensed Matter*. 2011; 406:972-980.

24. Efimov AM, Kostyreva TG and Sycheva GA. Water-related IR absorption spectra for alkali zinc pyrophosphate glasses. *Journal of Non-Crystalline Solids*. 1998; 238:124-142.

25. O'Donnell MD, Miller CA, Furniss D, Tikhomirov VK and Seddonet AB. Fluorotellurite glasses with improved mid-infrared transmission. *Journal of Non-Crystalline Solids*. 2003; 331:48-57.

26. Massera J, Haldeman A, Jackson J, Rivero-Baleine C, Petit L. and Richardson K. Processing of tellurite-based glass with low OH content. *Journal of the American Ceramic Society*. 2011; 94(1):130-136.